RESEARCH ARTICLE

Mycobacterial Esx-3 Requires Multiple Components for Iron Acquisition

M. Sloan Siegrist,[a] Magnus Steigedal,[a,b,c] Rushdy Ahmad,[d] Alka Mehra,[e] Marte S. Dragset,[a,b,c,f] Brian M. Schuster,[a] Jennifer A. Philips,[e] Steven A. Carr,[d] Eric J. Rubin[a]

Department of Immunology and Infectious Diseases, Harvard School of Public Health, Boston, Massachusetts, USA[a]; Department of Cancer Research and Molecular Medicine, Centre of Molecular Inflammation Research, Norwegian University of Science and Technology, Trondheim, Norway[b]; St. Olav's University Hospital, Trondheim, Norway[c]; Broad Institute of MIT and Harvard, Cambridge, Massachusetts, USA[d]; Division of Infectious Diseases, Department of Medicine, New York University School of Medicine, New York, New York, USA[e]; Department of Biotechnology, Norwegian University of Science and Technology, Trondheim, Norway[f]

ABSTRACT **The type VII secretion systems are conserved across mycobacterial species and in many Gram-positive bacteria. While the well-characterized Esx-1 pathway is required for the virulence of pathogenic mycobacteria and conjugation in the model organism *Mycobacterium smegmatis*, Esx-3 contributes to mycobactin-mediated iron acquisition in these bacteria. Here we show that several Esx-3 components are individually required for function under low-iron conditions but that at least one, the membrane-bound protease $MycP_3$ of *M. smegmatis*, is partially expendable. All of the *esx-3* mutants tested, including the Δ$mycP_{3ms}$ mutant, failed to export the native Esx-3 substrates $EsxH_{ms}$ and $EsxG_{ms}$ to quantifiable levels, as determined by targeted mass spectrometry. Although we were able to restore low-iron growth to the *esx-3* mutants by genetic complementation, we found a wide range of complementation levels for protein export. Indeed, minute quantities of extracellular $EsxH_{ms}$ and $EsxG_{ms}$ were sufficient for iron acquisition under our experimental conditions. The apparent separation of Esx-3 function in iron acquisition from robust $EsxG_{ms}$ and $EsxH_{ms}$ secretion in the Δ$mycP_{3ms}$ mutant and in some of the complemented *esx-3* mutants compels reexamination of the structure-function relationships for type VII secretion systems.**

IMPORTANCE **Mycobacteria have several paralogous type VII secretion systems, Esx-1 through Esx-5. Whereas Esx-1 is required for pathogenic mycobacteria to grow within an infected host, Esx-3 is essential for growth *in vitro*. We and others have shown that Esx-3 is required for siderophore-mediated iron acquisition. In this work, we identify individual Esx-3 components that contribute to this process. As in the Esx-1 system, most mutations that abolish Esx-3 protein export also disrupt its function. Unexpectedly, however, ultrasensitive quantitation of Esx-3 secretion by multiple-reaction-monitoring mass spectrometry (MRM-MS) revealed that very low levels of export were sufficient for iron acquisition under similar conditions. Although protein export clearly contributes to type VII function, the relationship is not absolute.**

Received 19 March 2014 **Accepted** 28 March 2014 **Published** 6 May 2014

Citation Siegrist MS, Steigedal M, Ahmad R, Mehra A, Dragset MS, Schuster BM, Philips JA, Carr SA, Rubin EJ. 2014. Mycobacterial Esx-3 requires multiple components for iron acquisition. mBio 5(3):e01073-14. doi:10.1128/mBio.01073-14.

Editor John Mekalanos, Harvard Medical School

Address correspondence to Eric J. Rubin, erubin@hsph.harvard.edu.

One of the many strategies evolved by *Mycobacterium tuberculosis* to prevent clearance by the host is protein export via Esx-1 (1–3), a specialized secretion system that is also required for conjugation in *M. smegmatis* (4, 5). There are four paralogous *esx* loci in the *M. tuberculosis* genome (6–8), but the functions of these Esx systems are just beginning to be revealed (9–19, 55).

Whereas Esx-1 is essential for the *in vivo* growth of pathogenic mycobacteria, there is strong evidence that Esx-3 is essential for *in vitro* growth (12, 13, 19, 20). Building on observations that *esx-3* expression responds to iron and zinc availability (21, 22), we and others have demonstrated that Esx-3 is required for mycobacterial growth in low iron (12, 13, 19). Mycobacteria acquire iron by at least two siderophore pathways—exochelin, present in fast-growing species, such as *M. smegmatis*, and mycobactin, present in nearly all species (23–25)—in addition to a porin-based, low-affinity iron transport system (26) and the heme uptake system (27, 28). Epistasis experiments using *M. smegmatis* strains with deficiencies in Esx-3 and in the production of exochelin or mycobactin show that Esx-3 functions in iron acquisition via the mycobactin pathway (13). Moreover, addition of purified, iron-bound mycobactin does not rescue the low-iron growth defect, suggesting that Esx-3 is required for optimal utilization of the siderophores (13).

The organizations and contents of the *esx-1* and *esx-3* loci are similar (8). Both encode small, secreted proteins; Esx-1 contains EsxB (Cfp-10) and EsxA (Esat-6), and Esx-3 contains the paralogous EsxG and EsxH proteins (Fig. 1). We use the systematic nomenclature proposed by Bitter et al. (29). Genes that flank *esxB/A* and *esxG/H* include those encoding $EccC_3$ (a putative FtsK/SpoIIIE ATPase that is paralogous to $EccCa_1$/$EccCb_1$ [where the "a" and "b" suffixes indicate the parts of the split gene and the subscript number refers to the *esx-1* gene cluster]), $EspG_3$ (a putative soluble protein of unknown function that is paralogous to $EspG_1$), $EccD_3$ (paralogous to the hypothesized secretion channel

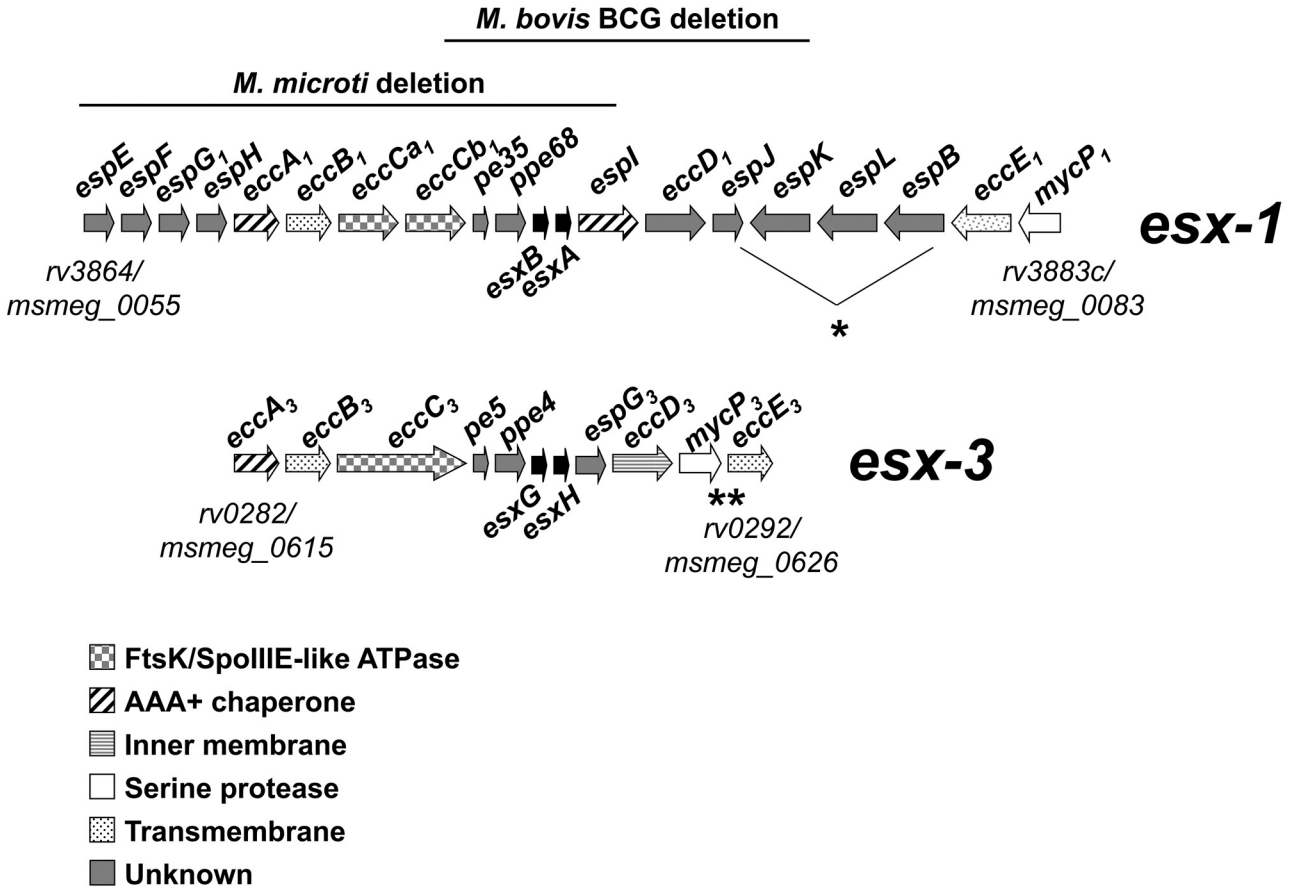

FIG 1 Schematic diagram of gene conservation in mycobacterial *esx-1* and *esx-3* loci. *, the *M. smegmatis esx-1* locus has a slightly different organization than the *M. tuberculosis* region from *espJ* to *espB* (5, 8); **, there is no *MSMEG_0625*, $mycP_{3ms}$ is *MSMEG_0624*, and $eccE_{3ms}$ is *MSMEG_0626*. We use the nomenclature proposed by Bitter et al. (29). Briefly, the terms *ecc* and *esp*, respectively, stand for *esx* conserved component and Esx-1 secretion-associated protein. The alphabetic suffix of conserved *esx* genes follows the gene order in the *esx-1* locus. The numerical subscript at the end of the gene name refers to the *esx* cluster to which the gene belongs. We also provide the standard *M. tuberculosis* and *M. smegmatis* gene numbers at the beginning and end of each locus for comparison. Although not listed in the NCBI or SmegmaList databases, *MSMEG_0620* is $esxG_{ms}$ and *MSMEG_0621* is $esxH_{ms}$.

protein $EccD_1$), and $MycP_3$ (paralogous to the membrane-bound protease $MycP_1$) (8).

Multiple studies on the Esx-1 system support a model in which the FtsK/SpoIIIE ATPase $EccCa_1/EccCb_1$ provides energy to propel EsxB and EsxA across the cytoplasmic membrane via a translocation pore composed of $EccD_1$ (30–32). It is not yet clear how type VII substrate proteins cross the cell envelope. Esx-1 may simply export these proteins across the cell envelope into the extracellular space. Alternatively, it may act only across the cytoplasmic membrane and require a mechanism for driving substrates across the remainder of the thick mycobacterial cell wall. Such a structure may be composed of yet-unidentified components or of EsxA, EsxB, and possibly other unlinked Esx-1 substrates (33, 34).

$EspG_1$, $EccCa_1/EccCb_1$, $EccD_1$, and $MycP_1$ are required for both EsxB and EsxA export and Esx-1 function in most mycobacterial species tested (3, 5, 35–41), prompting early speculation that EsxB and EsxA are the effector proteins of the secretion system. However, there have since been reports of several Esx-1 mutations that abolish function without affecting EsxB and EsxA export (4, 35, 42, 43), as well as two genetic perturbations that prevent *M. tuberculosis* EsxB ($EsxB_{mt}$) and $EsxA_{mt}$ secretion but do not alter *M. tuberculosis* virulence (44). These studies suggest that the relationship between protein export and Esx function may be more complicated than previously assumed.

Esx-3 exports EsxH (13) and, as we show here, EsxG. We found that several *M. smegmatis* Esx-3 components were individually required for export of $EsxH_{ms}$ and $EsxG_{ms}$ and for iron acquisition. However, we also observed low or even no detectable secretion for some strains that were able to grow to wild-type levels in low iron. The apparent separation of the phenotypes suggests new models for the associations between Esx structure and function.

RESULTS

Esx-3 components are required for low-iron growth. We have previously shown that Esx-3 is required for mycobacterial growth in low-iron medium via the mycobactin pathway (13). The secretion system is essential for growth in *M. tuberculosis* (12, 13, 20), however, complicating efforts to test the contributions of individual Esx-3 components to the function of the entire system. The model organism *M. smegmatis* can grow without functional Esx-3 in normal growth medium. We therefore constructed unmarked, in-frame deletions of *esx-3* genes in *M. smegmatis* (see Fig. S1 in the supplemental material). Because *M. smegmatis* has partially redundant siderophore-based iron acquisition mechanisms, i.e.,

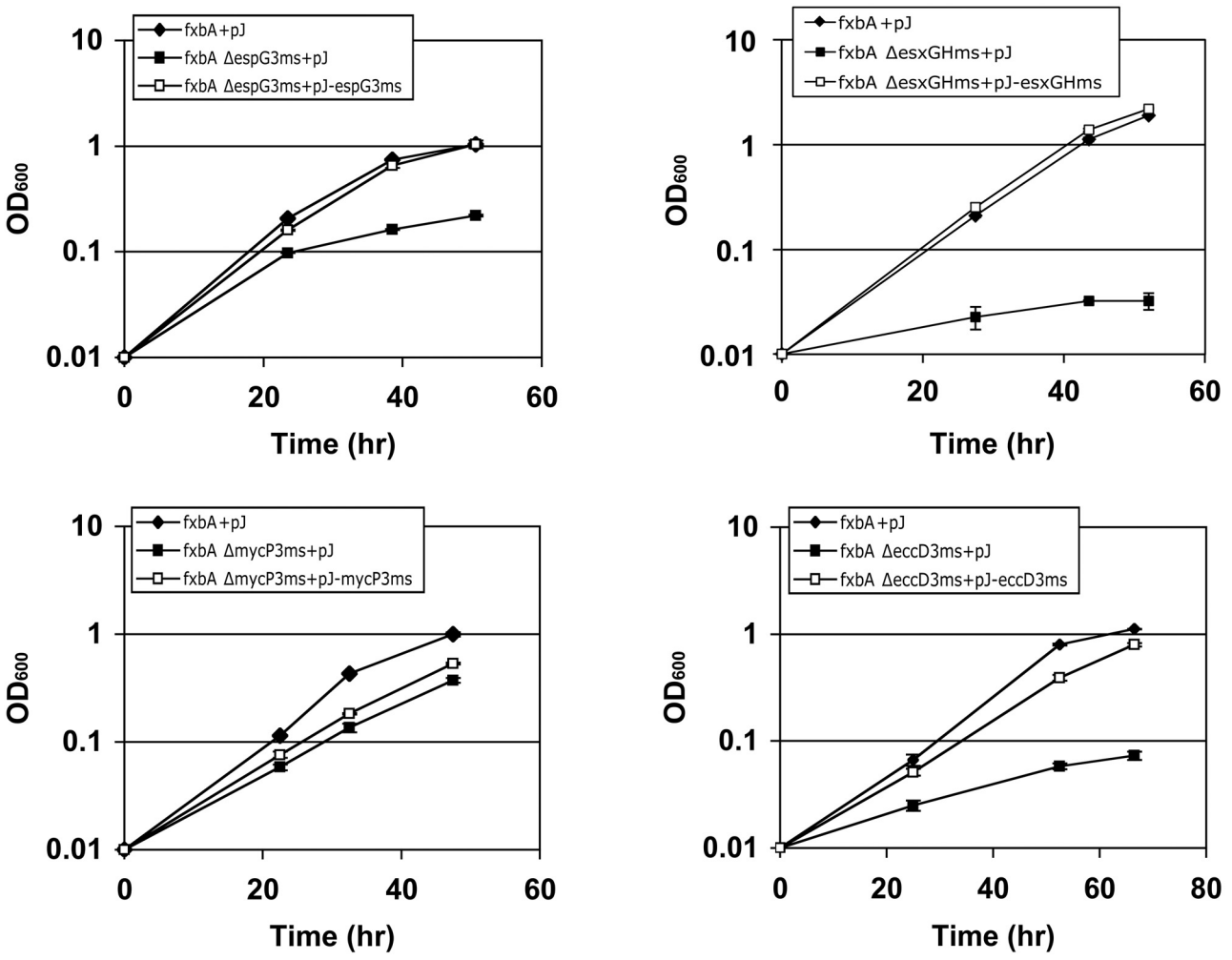

FIG 2 Esx-3 components contribute to low-iron growth. The growth of the *fxbA* and *fxbA esx-3 M. smegmatis* mutants in low-iron medium was monitored by determining their optical densities at 600 nm. pJ, pJEB402 vector; pJ-[gene name], pJEB402 containing the indicated *M. smegmatis* gene. The experiments were performed 2 to 6 times in triplicate. Representative data are shown, and error bars represent the standard deviations from the replicates.

the mycobactin and exochelin pathways (24), we combined each *esx-3* deletion with an insertional mutation in *fxbA*, which encodes a formyl transferase required for exochelin synthesis. Previously, we found that the *fxbA* Δ$eccC_{3ms}$ mutant grows significantly more slowly than the *fxbA* strain in low-iron medium (13). Although the *fxbA* Δ$esxGH_{ms}$, *fxbA* Δ$espG_{3ms}$, and *fxbA* Δ$eccD_{3ms}$ mutants display similar low-iron growth deficiencies, the *fxbA* Δ$mycP_{3ms}$ strain has a less pronounced defect (Fig. 2 and 3). These strains are rescued by the presence of iron (Fig. S2) and upon reintroduction of the corresponding *esx-3* gene (13) (Fig. 2). Thus, *M. smegmatis* growth in low iron requires the Esx-3 components $EccC_{3ms}$, $EsxG_{ms}$/$EsxH_{ms}$, $EspG_{3ms}$, and $EccD_{3ms}$, with a more minor contribution from $MycP_{3ms}$.

Esx-3 components contribute to optimal mycobactin utilization. Previously, we constructed an *M. smegmatis* strain that contains insertions in both *fxbA*, described above, and *mbtD*, which encodes a polyketide synthase required for mycobactin synthesis (13). This mutant, which lacks both means of high-affinity iron uptake, does not grow in iron-depleted medium but can be rescued by the addition of purified, iron-bound mycobactin or carboxymycobactin (13). However, the siderophores fail to rescue the *fxbA* Δ*esx-3* mutant, suggesting that Esx-3 is required for optimal utilization of iron bound to mycobactins (13). In the absence of the exochelin pathway, deletion of the *esx-3* gene $eccC_{3ms}$, $esxGH_{ms}$, $espG_{3ms}$, or $eccD_{3ms}$ impairs iron-bound mycobactin utilization in *M. smegmatis* to an extent similar to that after removal of the entire Esx-3 system, whereas deletion of $mycP_{3ms}$ has a more modest effect (Fig. 3). We conclude that the Esx-3 components $EccC_{3ms}$, $EsxG_{ms}$/$EsxH_{ms}$, $EspG_{3ms}$, and $EccD_{3ms}$ are critical to the function of the *M. smegmatis* Esx-3 system in mycobactin-mediated iron acquisition.

Secretion of $EsxH_{ms}$ and $EsxG_{ms}$ requires Esx-3 components. Secretion of EsxB and EsxA is generally linked to Esx-1 function; that is, most mutations that abolish export of these proteins also inhibit virulence (*M. tuberculosis* and *M. marinum*) or conjugation (*M. smegmatis*) (3–5, 35–40). Our work on the Esx-3 system demonstrates that $EccC_{3ms}$, $EsxG_{ms}$/$EsxH_{ms}$, $EspG_{3ms}$, and $EccD_{3ms}$ are required for function in mycobactin-mediated iron acquisition and that $MycP_{3ms}$ plays a more limited role (Fig. 2 and 3). Previously, we showed that export of heterologously expressed, myc-tagged EsxH depends on iron levels and on the presence of an intact Esx-3 locus (13). To test whether the loss of individual Esx-3

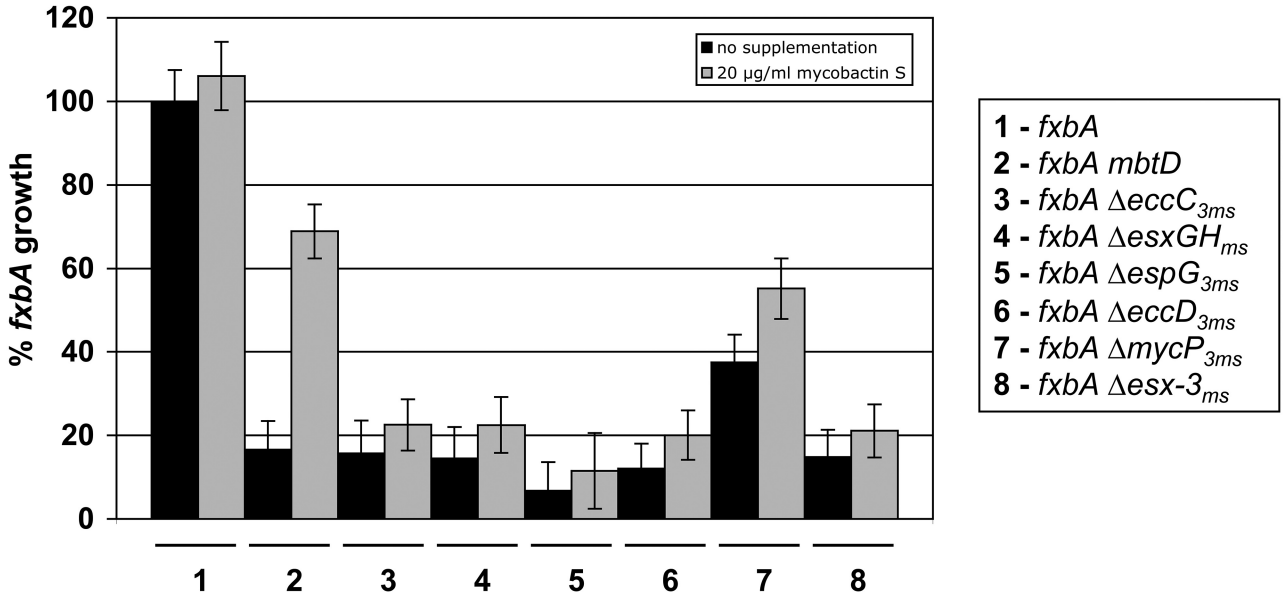

FIG 3 Loss of Esx-3 components is not rescued by exogenous mycobactin. Growth of *fxbA*, *fxbA mbtD*, and *fxbA esx-3* mutants in unsupplemented, low-iron medium or in low-iron medium containing 20 μg/ml mycobactin S at 48 h. The experiment was performed at least three times in triplicate. Representative data are shown and are expressed as percentages of the *fxbA* mutant's growth in low-iron medium. Error bars indicate the standard errors of the proportions.

components similarly influences protein export, we monitored the abundance of representative $EsxG_{ms}$ and $EsxH_{ms}$ peptides in culture filtrates and selected whole-cell extracts by targeted, quantitative mass spectrometry (MS). Assays for peptides from each of these proteins were constructed using stable-isotope dilution MS (SID-MS) and multiple-reaction-monitoring MS (MRM-MS) (45, 46). For these experiments, we grew strains with intact exochelin production in medium with a level of iron chelation that induces EsxH secretion (13) but does not produce differences in growth. Deletion of the *esx-3* gene $eccC_{3ms}$, $esxGH_{ms}$, $espG_{3ms}$, or $eccD_{3ms}$ results in supernatant levels of $EsxH_{ms}$ and $EsxG_{ms}$ that are below the limit of quantitation (LOQ) across two biological replicates (Fig. 4 and S3 to S5 in the supplemental material). Interestingly, although the $mycP_{3ms}$ mutation causes a much smaller defect in low-iron growth than the other mutations (Fig. 2), there is a comparable decrease in supernatant peptides in three of the four data sets to levels below the LOQ (Fig. 4 and S3 to S5).

We find most of the detectable $EsxH_{ms}$ and $EsxG_{ms}$ in the supernatant fraction of wild-type *M. smegmatis* (Fig. 4 and S5). To test whether the observed lack of secretion by the *esx-3* mutants reflects a general decrease in protein expression, we also compared the whole-cell extracts of the wild type, Δ$espG_{3ms}$ mutant, and complemented Δ$espG_{3ms}$ strain. The amounts of $EsxH_{ms}$ and $EsxG_{ms}$ were similar across the samples (Fig. S5), suggesting that the observed change in supernatant abundance accurately reports an export defect. The general lack of protein accumulation in the whole-cell extract, furthermore, implies that the cell tightly regulates the abundance of what we hypothesize is a small, cytoplasmic pool of $EsxH_{ms}$ and $EsxG_{ms}$.

These data were consistent with our previous findings that Esx-3 is required for the export of $EsxH_{ms}$-myc (13). Unlike native $EsxG_{ms}$ and $EsxH_{ms}$, however, the tagged protein accumulates in the bacterial cytoplasm to robust levels (13). Therefore, we confirmed the mass spectrometry findings by constructing a new plasmid that constitutively expresses $esxG_{ms}$ and FLAG-tagged $esxH_{ms}$ and comparable amounts of $EsxH_{ms}$-FLAG in cell-associated and supernatant fractions of wild-type and *esx-3* mutant *M. smegmatis* strains. In agreement with the MRM-MS results, we were consistently unable to detect $EsxH_{ms}$-FLAG from the supernatants of the Δ$eccC_{3ms}$, Δ$espG_{3ms}$, Δ$eccD_{3ms}$, and Δ$mycP_{3ms}$ mutants or from any of the whole-cell extracts (Fig. 5).

DISCUSSION

We found that $EccC_{3ms}$, $EspG_{3ms}$, and $EccD_{3ms}$ are core Esx-3 components that are required for both mycobactin-mediated iron acquisition and $EsxG_{ms}$ and $EsxH_{ms}$ export. The *M. tuberculosis* homologs $EccC_{3mt}$, $EspG_{3mt}$, and $EccD_{3mt}$ are all predicted to be necessary for *in vitro* growth (20, 47, 48). The Esx-1 paralogs $EccCa_1$/$EccCb_1$, $EspG_1$, and $EccD_1$ are required for virulence in pathogenic mycobacteria and conjugation in *M. smegmatis* and, with the exception of $EspG_{1mt}$ (35, 42), for EsxB and EsxA export (3–5, 35–40).

We have also identified a potential accessory Esx-3 component, $MycP_3$, that is necessary for EsxG and EsxH export (Fig. 4 and 5) but not absolutely required for mycobactin-mediated iron acquisition (Fig. 2 and 3). The first observation is not unexpected, as mutants that lack $MycP_1$ fail to secrete EsxB and EsxA (36, 41). The data on the contribution of MycP to Esx function are less clear; although $MycP_{1ms}$ is required for DNA transfer in *M. smegmatis* to the same or greater extent as other Esx-1 components (4, 36), $mycP_{1mt}$ disruption in *M. tuberculosis* results in a delayed phenotype in mice compared to the phenotypes resulting from transposon insertions in other *esx-1* genes (49). More recent work corroborates an *in vivo* growth defect from loss of $MycP_{1mt}$ (41), but the lack of a direct comparison to other *esx-1* mutant strains precluded analysis of the relative defect. Like the other *esx-3* genes, $mycP_{3mt}$ is essential for *M. tuberculosis* growth *in vitro* (47). Given that $MycP_1$ and $MycP_3$ likely have different substrate specificities

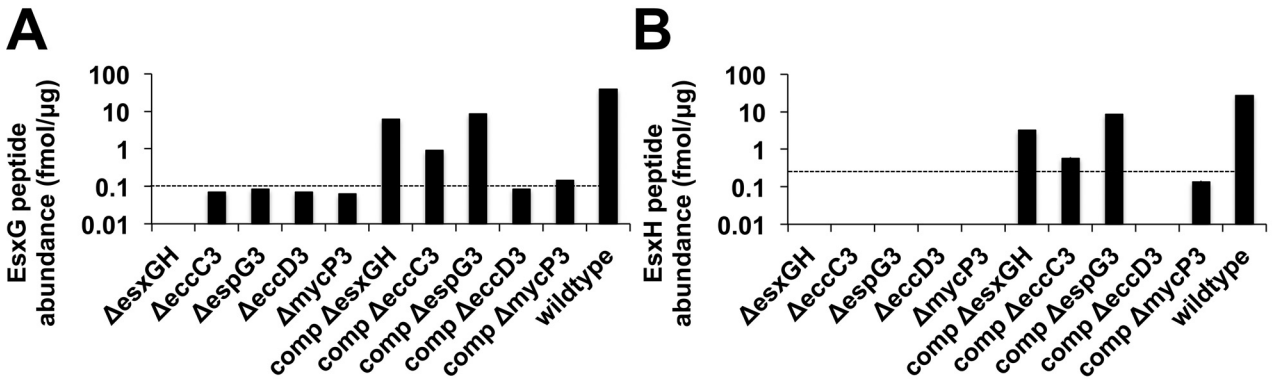

$EsxG_{ms}$: FVEVSAK		
Sample	Concentration	
	fmol/µg	pg/µg
ΔesxGH$_{ms}$	ND	ND
Δ*eccC*$_{3ms}$	0.071 +/- 0.002	0.706 +/- 0.019
Δ*espG*$_{3ms}$	0.084 +/- 0.002	0.835 +/- 0.019
Δ*eccD*$_{3ms}$	0.071 +/- 0.001	0.706 +/- 0.009
Δ*mycP*$_{3ms}$	0.062 +/- 0.001	0.616 +/- 0.009
comp *ΔesxGH*$_{ms}$	6.16 +/- 0.12	61.21 +/- 1.23
comp Δ*eccC*$_{3ms}$	0.899 +/- 0.015	8.94 +/- 0.15
comp Δ*espG*$_{3ms}$	8.527 +/- 0.223	84.76 +/- 2.22
comp Δ*eccD*$_{3ms}$	0.085 +/- 0.002	0.845 +/- 0.019
comp Δ*mycP*$_{3ms}$	0.145 +/- 0.005	1.44 +/- 0.05
wildtype	38.96 +/- 0.70	387.24 +/- 6.99

$EsxH_{ms}$: AMATTHEQNTMAMSAR		
Sample	Concentration	
	fmol/µg	pg/µg
ΔesxGH$_{ms}$	ND	ND
Δ*eccC*$_{3ms}$	ND	ND
Δ*espG*$_{3ms}$	ND	ND
Δ*eccD*$_{3ms}$	ND	ND
Δ*mycP*$_{3ms}$	ND	ND
comp *ΔesxGH*$_{ms}$	3.18 +/- 0.14	33.27 +/- 1.45
comp Δ*eccC*$_{3ms}$	0.579 +/- 0.031	6.06 +/- 0.33
comp Δ*espG*$_{3ms}$	8.50 +/- 0.07	88.96 +/- 0.69
comp Δ*eccD*$_{3ms}$	ND	ND
comp Δ*mycP*$_{3ms}$	0.133 +/- 0.010	1.39 +/- 0.11
wildtype	26.86 +/- 0.45	281.22 +/- 4.74

FIG 4 $EsxG_{ms}$ (A) and $EsxH_{ms}$ (B) abundances in wild-type and *esx-3* mutant supernatants. Protein concentrations for $EsxG_{ms}$ and $EsxH_{ms}$ were approximated, respectively, by measuring the concentration of the FVEVSAK peptide alone and by summing the individual concentrations above the LOD of three of the methionine forms of AMATTHEQNTMAMSAR peptides (Fig. S4). Dotted lines show the LOQ (Fig. S4). The experiments were performed in technical replicate across two biological replicates. The protein abundance data from one of the biological replicates are shown here in graphical and table format, and the data from the other replicate are reported in the Fig. S5 table. comp, complemented; ND, none detected.

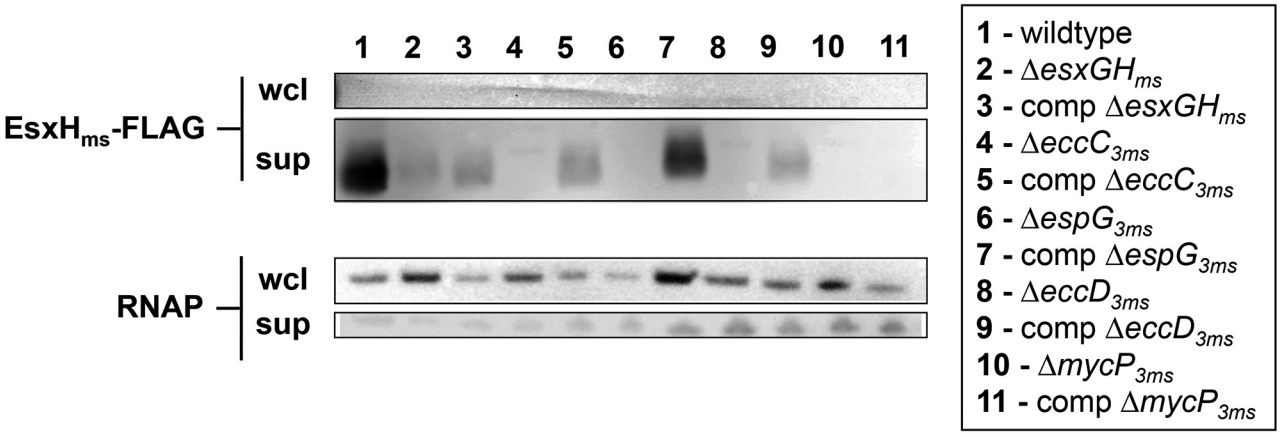

FIG 5 Export of epitope-tagged $EsxH_{ms}$ in the presence or absence of Esx-3 components. Anti-FLAG immunoblotting of whole-cell lysates (wcl) and culture supernatants (sup) from wild-type and *esx-3 M. smegmatis* containing pSYMP-*esxGH*$_{ms}$-FLAG in low-iron medium. All strains contain either the empty pJEB402 vector or pJEB402 containing the complementing gene. The antibody against the intracellular protein RNAP is a loading and lysis control. The experiment was performed twice with similar results.

(41, 50, 51), it may be that the relative importance of MycP as an Esx component varies according to the secretion apparatus with which it associates.

Despite our attempts to avoid polar effects by constructing in-frame, unmarked, full gene deletions, it is possible that the mutations altered the expression of downstream genes. However, this does not appear to be the case for at least the Δ*mycP*$_{3ms}$ mutant, as neither *mycP*$_{3ms}$ alone nor *mycP*$_{3ms}$ alongside the downstream *eccE*$_{3ms}$ restored EsxH$_{ms}$-FLAG export (not shown). Transcription of the *esx-3* locus varies according to iron and zinc availability (13, 21, 22). It is possible that expression of the complementing genes from a heterologous, constitutive promoter altered the stoichiometry of Esx-3 components, which in turn resulted in suboptimal protein secretion.

We attempted to measure secreted proteins using native antibodies and Western blotting. However, the antisera that we were able to obtain had low affinity and poor specificity, making quantitation difficult. Given the tendency of secretion systems to be refractory to reporter fusions (52), we turned to MRM-MS to measure bacterial protein export. This label-free method is highly specific and sensitive and is likely to have broad applicability to bacterial protein secretion studies (53).

Precise quantitation of secretion by MRM-MS revealed a surprising dynamic range in the levels of EsxG and EsxH export that support iron acquisition. We were able to restore *esx-3* mutant growth to wild-type levels by adding iron to the growth medium (Fig. S2) or by complementing the deleted genes (Fig. 2). However, the same genetic constructs varied widely in their abilities to restore EsxG$_{ms}$ and EsxH$_{ms}$ export (Fig. 4 and 5). Only a fraction of secreted wild-type EsxG$_{ms}$ and EsxH$_{ms}$ levels appeared necessary for complementation; we observed robust low-iron growth (Fig. 2) concomitant with protein export that spanned 3 orders of magnitude, from <1% to approximately 40% of wild-type levels (Fig. 4). We recently found that the essential drug targets dihydrofolate reductase and D-alanine racemase are present in excess (54). It is possible that wild-type *M. smegmatis* exports EsxG$_{ms}$ and EsxH$_{ms}$ at levels much greater than those needed to support low-iron growth. This raises the possibility that the locus has multiple functions, each with different secretion requirements.

Indeed, there is growing appreciation that the relationship between Esx protein export and function is more complex than initially assumed. There are now numerous reports of Esx-1 mutations that attenuate pathogenic mycobacteria without impacting secretion. For example, complementation of the natural *esx-1* mutant *M. microti* (Fig. 1) with a panel of cosmids containing intact or mutant versions of the *M. tuberculosis esx-1* region revealed that *espF*$_{1mt}$ and *espG*$_{1mt}$ are required for virulence but not EsxB$_{mt}$ and EsxA$_{mt}$ export (35). Deletion of these genes from *M. tuberculosis* also resulted in attenuation without impacting the secretion of EsxB$_{mt}$ and EsxA$_{mt}$ (42). In a different example, disruption of disulfide bond formation in the Esx-1 substrate EspA attenuated *M. tuberculosis* virulence but had no effect on EsxB$_{mt}$ or EsxA$_{mt}$ secretion (43). Finally, transposon insertions in *espJ*$_{ms}$, *espK*$_{ms}$, and *espB*$_{ms}$ impaired conjugation but not EsxB$_{ms}$ export (4). In aggregate, these studies show that secretion of EsxB and EsxA is not sufficient for Esx-1 function in virulence.

Recently, Chen and coworkers isolated two point mutations of EspA$_{mt}$ that block EsxB$_{mt}$ and EsxA$_{mt}$ export *in vitro* but do not attenuate *M. tuberculosis* (44). Although they did not rule out a role for the host environment in permitting secretion *in vivo*, these data suggest that export of these proteins, at least in large amounts, may not be strictly required for virulence. Similarly, we found a mutation that inhibits Esx protein secretion but permits partial function: loss of *mycP*$_{3ms}$ blocked the export of native EsxG$_{ms}$ and EsxH$_{ms}$ and FLAG-tagged EsxH$_{ms}$ (Fig. 4 and 5), yet the *fxbA* Δ*mycP*$_{3ms}$ mutant retained some ability to grow in low iron (Fig. 2). We also found that very low quantities of EsxG$_{ms}$ and EsxH$_{ms}$ secretion were sufficient to reinstate low-iron growth to some of our complemented *esx-3* mutants (Fig. 2 and 4). Importantly, dissection of the Esx-3 system in the model organism *M. smegmatis* allowed us to compare the two phenotypes, EsxG and EsxH export and mycobactin-mediated iron acquisition, under similar *in vitro* conditions.

Why are not protein secretion and iron utilization completely congruent in our mutant strains? This is especially puzzling given that the genome of *M. smegmatis*, unlike *M. tuberculosis*, does not encode the closely related paralogs EsxR and EsxS, which might otherwise be hypothesized to substitute for EsxG and EsxH function (8). One reason may be the existence of multiple Esx substrates, each with its own requirements for export and contributions to function. The roles of EspG and EspB are particularly informative in this regard. Inactivation of the paralogous *espG*$_1$, *espG*$_5$, or, as we show in Fig. 4, *espG*$_3$ gene generally prevents the export of Esx substrate proteins (11, 17, 37, 42). However, in *M. tuberculosis*, loss of EspG$_{5mt}$ did not produce an obvious phenotype (55), while EspG$_{1mt}$ was required for full virulence but not EsxB$_{mt}$ or EsxA$_{mt}$ secretion (35, 42). Interestingly, EspG$_1$ and EspG$_5$ have been shown to interact specifically with cognate Pro-Glu (PE)/Pro-Pro-Glu (PPE) proteins (56, 57) and have been proposed to serve as chaperones for Esx secretion of these substrates (57). These data suggest that the PE/PPE proteins have export requirements and functional contributions distinct from those of other type VII substrates. Similarly, the secretion and activity of the Esx-1 substrate EspB appear to be independent of EsxA (58, 59) and EsxB (60).

Our data are consistent with at least three general models. It is conceivable that loss of Esx-3 function produces global changes in cell wall structure such that protein localization is affected by changes both in secretion and in the compartment into which translocation occurs. We note that while *esx-3* mutants do not have altered sensitivities to SDS, vancomycin, rifampin (Fig. S5), ampicillin, or kanamycin (19), at least when iron is not limiting, we are unable to rule out this model. A second possibility is that Esx-3 secretes a protein or proteins necessary for iron acquisition and that this protein requires the core components EccC$_3$, EccD$_3$, and EspG$_3$ but not EsxG, EsxH, or MycP$_3$ for export. Although it is possible that Esx-3 function in iron acquisition does not require any EsxG and EsxH secretion, we think that this is unlikely given that the *fxbA* Δ*esxGH*$_{ms}$ strain has a complementable growth phenotype in low iron. A third model is that both EsxG and EsxH are substrates and structural components of or chaperones for the Esx-3 machinery. In this scenario, EsxG and EsxH are exported across the cytoplasmic membrane via EccD$_3$ into the periplasm, where they are poised to deliver yet-unidentified effectors of ferrimycobactin uptake across the remainder of the cell wall (Fig. 6). If EsxG and EsxH indeed act within or across the mycobacterial envelope, some of the protein detected in the supernatants of broth-grown mycobacteria may represent sloughing of protein associated with the cell wall (33, 34).

While type VII secretion systems have important functions

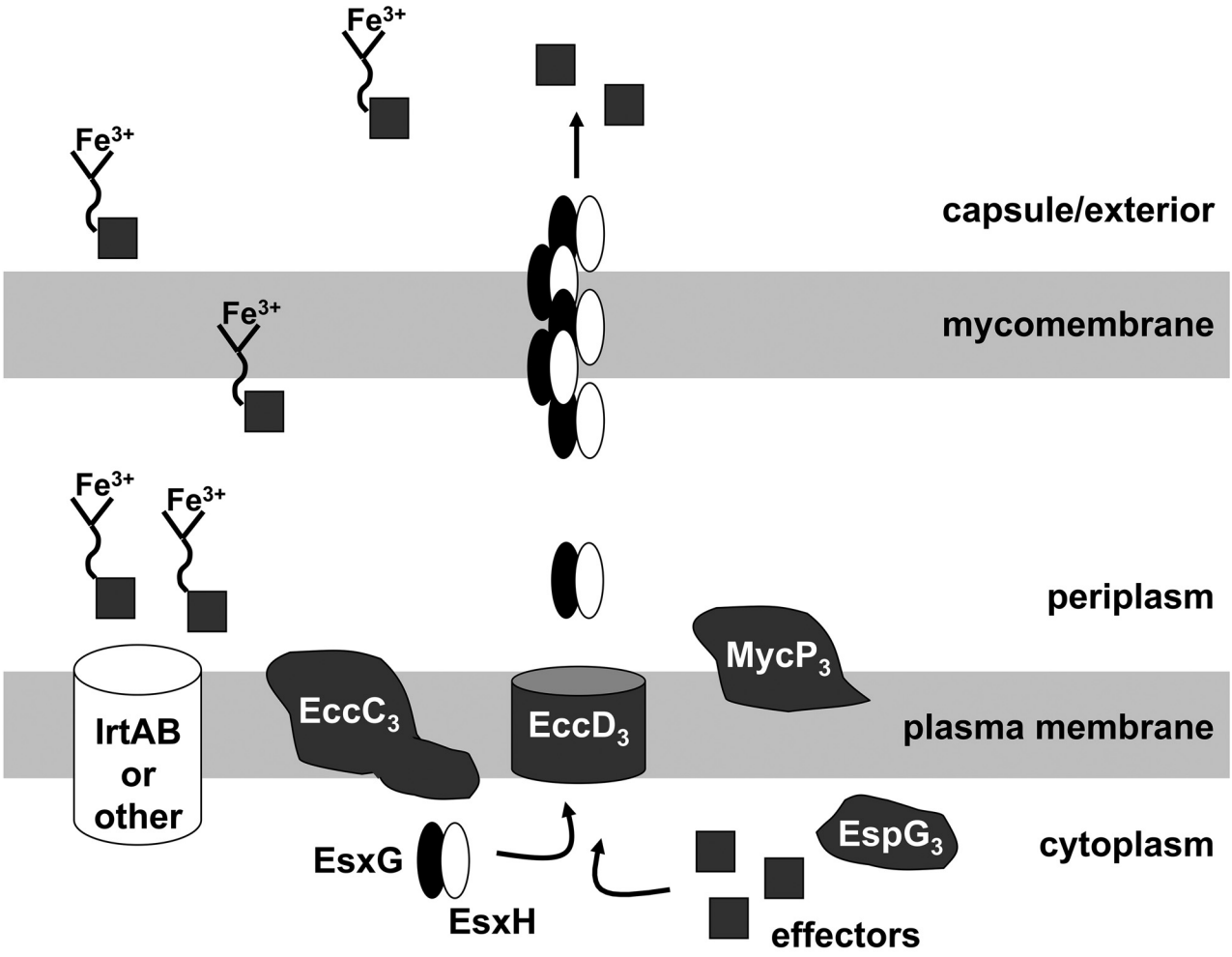

FIG 6 One model for Esx-3 function in which EsxG and EsxH are both substrates and chaperones or structural components of the secretion apparatus. IrtA and IrtB are components of a mycobactin transporter system (63–65). We hypothesize that at least one of the functions of EsxG and EsxH is to ferry effectors of iron-loaded mycobactin uptake within or across the mycobacterial cell wall. In the absence of an Esx-3 core component, such as $EccD_3$, we do not detect EsxG or EsxH in culture supernatants. We hypothesize that the proteins are not exported across the cytoplasmic membrane under this condition and therefore are completely unable to contribute to iron acquisition. In contrast, although supernatants from *fxbA* $\Delta mycP_{3ms}$ cultures do not contain detectable EsxG or EsxH, the strain itself retains intermediate growth under low-iron conditions. We suggest the $MycP_3$ protease may be an accessory Esx-3 component that is required either for a stable EsxG-EsxH structure or for optimal chaperone activity. Thus, in the absence of this accessory factor, EsxG and EsxH may still traverse the cytoplasmic membrane to the periplasm but be only partially functional.

both *in vitro* and *in vivo*, their molecular mechanisms remain unclear. Clearly, protein export contributes to but does not entirely account for type VII function. More complete models for type VII structure-function relationships will require better characterization of secreted components and assays for protein-protein interactions that occur between Esx components in the cytosol or membrane (55, 61).

MATERIALS AND METHODS

Bacterial strains and growth conditions. *M. smegmatis* was cultured in chelated Sauton's medium containing 60 ml glycerol, 0.5 g KH_2PO_4, 2.2 g citric acid monohydrate, 4 g asparagine, and 0.05% Tween 80 per liter. After adjusting the pH to 7.4, the medium was stirred for 1 to 2 days at room temperature with 10 g Chelex 100 resin (Sigma). The medium was filtered, and 1 g $MgSO_4 \cdot 7H_2O$ was added as a sterile solution. For iron starvation experiments, bacteria were first inoculated from frozen stocks into 7H9 medium, subcultured once in chelated Sauton's medium, and then diluted 1:1,000 in chelated Sauton's medium without antibiotics containing either 100 μM 2,2′-dipyridyl or 12.5 μM $FeCl_3$. For mycobactin complementation experiments, bacteria were directly diluted 1:1,000 from a 7H9 starter culture into chelated Sauton's medium with or without ferri-mycobactin S.

Strain construction. To create the *M. smegmatis esx-3* gene deletions, 1-kb regions flanking $eccC_{3ms}$, $espG_{3ms}$, $eccD_{3ms}$, $mycP_{3ms}$, and $esxGH_{ms}$ were amplified from *M. smegmatis* genomic DNA, stitched together by PCR, and cloned into the suicide vector pJM1. The pJM1 vector contains a hygromycin-chloramphenicol resistance cassette and the counterselectable marker *sacB*. *M. smegmatis* transformants were screened by PCR using primers specific to the flanks as well as to regions within the putative deletion. Candidates were confirmed by PCR using multiple primers outside the flanks. To construct *fxbA* insertional mutants, the *esx-3* deletion strains were transformed with the pSES-*fxbA* suicide vector (13) and screened by standard methods. The absence of exochelin production was confirmed for candidate mutants by patching them to chrome azurol (CAS) agar.

Complementing constructs for each mutant were constructed by am-

plifying the regions from genomic *M. smegmatis* DNA and cloning them under the MOP promoter in the integrative pJEB402 plasmid (38). The construct containing $esxG_{ms}$ and $esxH_{ms}$ C-terminally tagged with FLAG was generated by amplifying the region from genomic *M. smegmatis* DNA and cloning it under the control of the *hsp60* promoter of pSYMP (62).

SID, MRM-MS. (i) Labeled-peptide internal standards. Figure S3 shows the amino acid sequences of the proteins $EsxG_{ms}$ and $EsxH_{ms}$ and the peptides that were selected for quantitative analysis of these proteins by multiple-reaction-monitoring mass spectrometry (MRM-MS). A peptide from each of the proteins was selected based on their detection in the discovery data by high electrospray MS signal responses and because they have unique sequences as determined by a search of the nonredundant *M. tuberculosis* protein database (NCBI nr). Four different versions of the peptide AMATTHEQNTMAMSAR for the $EsxH_{ms}$ protein were selected, all of which were observed in the discovery data.

(ii) Peptide synthesis. Five signature peptides from the two proteins, $EsxG_{ms}$ (FVEVSAK) and $EsxH_{ms}$ (AMATTHEQNTMAMSAR, with four forms of differing oxidized methionine states), were synthesized with a single, uniformly labeled [$^{13}C_6$]lysine or [$^{13}C_6$]arginine at their C termini by New England Peptide (Gardner, MA). Unlabeled ^{12}C-labeled forms of each peptide were also synthesized by New England Peptide. Synthetic peptides were purified to >99% purity and analyzed by amino acid analysis (New England Peptide). Calculations of concentrations were based upon amino acid analysis.

(iii) MRM-MS assay configuration. The limits of detection and quantification (LOD and LOQ, respectively) for the signature peptides used to obtain quantitative measurements in each of the 22 samples (5 mutants, 5 complemented mutants and 1 wild-type strain in each of two biological process replicates) are shown in Fig. S4. A 12-point response curve was generated by spiking light peptide versions of the 5 analyte peptides over a range of 0 to 50 fmol/1 μg of digested supernatant protein and a fixed amount of heavy, internal-standard peptides (1 fmol/1 μg) of the supernatant protein mix from the $\Delta esxGH_{ms}$ sample. This supernatant of the $\Delta esxGH_{ms}$ sample was used as the background matrix for response curve generation, as it does not express the proteins of interest. Each concentration point was analyzed by liquid chromatography (LC)–MRM-MS on a Waters Xevo TQ mass spectrometer (Milford, MA) in three technical replicates. The LOD was determined by the Linnet statistical method, and the lower LOQ was calculated as 3 times the LOD. The blank sample consists of the $\Delta esxGH_{ms}$ sample with only the isotopically labeled (heavy) peptides spiked in.

(iv) Nano-LC–MRM-MS. Tryptic peptides were prepared from culture supernatants (see below) and reconstituted in 80 μl of 0.1% formic acid, and 1 μg/μliter of each sample was used for MRM-MS analysis. Nano-LC–MRM-MS was performed on a Xevo TQ mass spectrometer (Waters Corporation, Milford, MA) coupled to a Nano Acuity LC system. Chromatography was performed with solvent A (0.1% formic acid) and solvent B (100% acetonitrile in 0.1% formic acid). Each sample was injected with a full-loop injection of 1 μl on a Waters, packed, Reprosil, 3-μm-bead column (75-μm internal diameter [ID], 10-μm ID tip opening) with a 2.5-in by 20-μm ID spray needle. Sample was eluted at 300 nl/min, with a gradient of 3 to 7% solvent B for 8 min, 7 to 40% solvent B for 34 min, and 40 to 90% solvent B for 3 min, with a total data acquisition time of 80 min. Data were acquired with a stable column temperature of 35°C. Collision energy (CE) was optimized for the maximum transmission and sensitivity of each MRM transition by LC–MRM-MS. Three transitions were monitored per peptide and acquired at unit resolution both in the first and in the third quadrupole (Q1 and Q3). In general, transitions were chosen based upon relative abundance and a mass-to-charge ratio (*m/z*) greater than the precursor *m/z* in the full-scan tandem MS (MS/MS) spectrum recorded on the Xevo TQ mass spectrometer. The final MRM-MS method consisted of 10 optimized transitions for each of the five selected peptides from the two target proteins. One of the four peptides (AMATTHEQNTMAMSAR) was not used for data analysis due to a weak signal.

(v) MRM-MS data analysis. Data analysis was performed using the Skyline Software Module (https://skyline.gs.washington.edu/). The relative ratios of the three transitions selected and optimized for the final MRM assay were predefined in the absence of the target proteins (i.e., in buffer) for each peptide using the ^{13}C-labeled internal standards. The most abundant transition for each pair was used for quantification unless interference in this channel was observed. The $^{12}C/^{13}C$ peak area ratios were used to calculate concentrations of the target peptides in each sample by the following equation: measured concentration = peak area ratio × (1 fmol/μl internal standard).

Sample preparation for MRM-MS analysis. Strains were inoculated from frozen stocks in 7H9 medium with appropriate antibiotics and grown with shaking for 48 h. The cells were then washed twice in chelated Sauton's medium, normalized by their optical densities at 600 nm (OD_{600}s), and inoculated 1:500 into chelated Sauton's medium. Cultures were grown for 48 h to log phase, and 8 OD units were harvested. Bacteria in the pellets were lysed by bead beating, and the lysates were stored at −80°C. Protein from the supernatant was precipitated by the trichloroacetic acid (TCA) method and dissolved in urea-ammonium-bicarbonate buffer (8 M urea, 50 mM ammonium bicarbonate). Protein concentration was measured by the Bradford assay of diluted samples.

One hundred micrograms of protein was reduced by 20 mM dithiothreitol (DTT) and alkylated using 50 mM iodoacetamide. Prior to being digested with trypsin, samples were diluted to a urea concentration of 0.6 M by the addition of 50 mM ammonium bicarbonate. Trypsin (Promega Gold) digestion was carried out at an enzyme-to-substrate ratio of 1:50. The peptides were desalted using Sep-Pak cartridges (Sep-Pak C_{18} 1-cc [50-mg] Vac cartridges; Waters) as described by the manufacturer. In the final step, samples were eluted in 80% acetonitrile and 0.1% formic acid and evaporated to complete dryness in a vacuum centrifuge.

Immunoblotting. Strains were inoculated from frozen stocks into 7H9 medium and grown to saturation. They were then diluted 1:500 in chelated Sauton's medium, grown to saturation, and diluted 1:100 in chelated Sauton's medium. Proteins from cell pellets and supernatants of cultures grown for 12 h in this fashion were run on 10 to 20% Tris-Tricine gels (Invitrogen) and revealed using an anti-FLAG antibody. An antibody to RNA polymerase (RNAP; Neoclone W0023), an intracellular protein, served as a loading and lysis control.

SUPPLEMENTAL MATERIAL

Supplemental material for this article may be found at http://mbio.asm.org/lookup/suppl/doi:10.1128/mBio.01073-14/-/DCSupplemental.

Figure S1, PDF file, 0.2 MB.
Figure S2, PDF file, 0.1 MB.
Figure S3, PDF file, 0.1 MB.
Figure S4, PDF file, 0.1 MB.
Figure S5, PDF file, 0.1 MB.
Figure S6, PDF file, 0.1 MB.

ACKNOWLEDGMENTS

We thank Colin Ratledge for providing ferri-mycobactin S and Jeff Murry for constructing the pJM1 vector. We gratefully acknowledge the helpful advice and insight from Meera Unnikrishnan, Sarah Fortune, and Jeff Murry. We also thank Mike Burgess for his help in running the MRM-MS assays.

This research was supported in part by the Broad Institute of MIT and Harvard (S.A.C.) and by grants to E.J.R. (NIH/NIAID grant 1P01 AI074805-01A1), J.A.P. (NIH/NIAID grant 1R01 AI087682-01A1 and a Clinical Scientist Development Award from the Doris Duke Charitable Foundation), and M.S. (Research Council of Norway grants 220836/H10 and 223255/F50).

REFERENCES

1. **Lewis KN, Liao R, Guinn KM, Hickey MJ, Smith S, Behr MA, Sherman DR.** 2003. Deletion of RD1 from *Mycobacterium tuberculosis* mimics

Bacille Calmette-Gu érin attenuation. J. Infect. Dis. **187:**117–123. http://dx.doi.org/10.1086/345862.

2. **Pym AS, Brodin P, Brosch R, Huerre M, Cole ST.** 2002. Loss of RD1 contributed to the attenuation of the live tuberculosis vaccines *Mycobacterium bovis* BCG and *Mycobacterium microti*. Mol. Microbiol. **46:** 709–717. http://dx.doi.org/10.1046/j.1365-2958.2002.03237.x.
3. **Pym AS, Brodin P, Majlessi L, Brosch R, Demangel C, Williams A, Griffiths KE, Marchal G, Leclerc C, Cole ST.** 2003. Recombinant BCG exporting ESAT-6 confers enhanced protection against tuberculosis. Nat. Med. **9:**533–539. http://dx.doi.org/10.1038/nm859.
4. **Coros A, Callahan B, Battaglioli E, Derbyshire KM.** 2008. The specialized secretory apparatus ESX-1 is essential for DNA transfer in *Mycobacterium smegmatis*. Mol. Microbiol. **69:**794–808. http://dx.doi.org/10.1111/j.1365-2958.2008.06299.x.
5. **Flint JL, Kowalski JC, Karnati PK, Derbyshire KM.** 2004. The RD1 virulence locus of *Mycobacterium tuberculosis* regulates DNA transfer in *Mycobacterium smegmatis*. Proc. Natl. Acad. Sci. U. S. A. **101:** 12598–12603. http://dx.doi.org/10.1073/pnas.0404892101.
6. **Cole ST, Brosch R, Parkhill J, Garnier T, Churcher C, Harris D, Gordon SV, Eiglmeier K, Gas S, Barry CE, III, Tekaia F, Badcock K, Basham D, Brown D, Chillingworth T, Connor R, Davies R, Devlin K, Feltwell T, Gentles S, Hamlin N, Holroyd S, Hornsby T, Jagels K, Krogh A, McLean J, Moule S, Murphy L, Oliver K, Osborne J, Quail MA, Rajandream MA, Rogers J, Rutter S, Seeger K, Skelton J, Squares R, Squares S, Sulston JE, Taylor K, Whitehead S, Barrell BG.** 1998. Deciphering the biology of *Mycobacterium tuberculosis* from the complete genome sequence. Nature **393:**537–544. http://dx.doi.org/10.1038/31159.
7. **Tekaia F, Gordon SV, Garnier T, Brosch R, Barrell BG, Cole ST.** 1999. Analysis of the proteome of *Mycobacterium tuberculosis* in silico. Tuber. Lung Dis. **79:**329–342. http://dx.doi.org/10.1054/tuld.1999.0220.
8. **Gey Van Pittius NC, Gamieldien J, Hide W, Brown GD, Siezen RJ, Beyers AD.** 2001. The ESAT-6 gene cluster of *Mycobacterium tuberculosis* and other high G+C Gram-positive bacteria. Genome Biol. **2:**RESEARCH0044. http://dx.doi.org/10.1186/gb-2001-2-10-research0044.
9. **Abdallah AM, Savage ND, van Zon M, Wilson L, Vandenbroucke-Grauls CM, van der Wel NN, Ottenhoff TH, Bitter W.** 2008. The ESX-5 secretion system of *Mycobacterium marinum* modulates the macrophage response. J. Immunol. **181:**7166–7175.
10. **Abdallah AM, Verboom T, Hannes F, Safi M, Strong M, Eisenberg D, Musters RJ, Vandenbroucke-Grauls CM, Appelmelk BJ, Luirink J, Bitter W.** 2006. A specific secretion system mediates PPE41 transport in pathogenic mycobacteria. Mol. Microbiol. **62:**667–679. http://dx.doi.org/10.1111/j.1365-2958.2006.05409.x.
11. **Abdallah AM, Verboom T, Weerdenburg EM, Gey van Pittius NC, Mahasha PW, Jiménez C, Parra M, Cadieux N, Brennan MJ, Appelmelk BJ, Bitter W.** 2009. PPE and PE_PGRS proteins of *Mycobacterium marinum* are transported via the type VII secretion system ESX-5. Mol. Microbiol. **73:**329–340. http://dx.doi.org/10.1111/j.1365-2958.2009.06783.x.
12. **Serafini A, Boldrin F, Palù G, Manganelli R.** 2009. Characterization of a *Mycobacterium tuberculosis* ESX-3 conditional mutant: essentiality and rescue by iron and zinc. J. Bacteriol. **191:**6340–6344. http://dx.doi.org/10.1128/JB.00756-09.
13. **Siegrist MS, Unnikrishnan M, McConnell MJ, Borowsky M, Cheng TY, Siddiqi N, Fortune SM, Moody DB, Rubin EJ.** 2009. Mycobacterial Esx-3 is required for mycobactin-mediated iron acquisition. Proc. Natl. Acad. Sci. U. S. A. **106:**18792–18797. http://dx.doi.org/10.1073/pnas.0900589106.
14. **Sweeney KA, Dao DN, Goldberg MF, Hsu T, Venkataswamy MM, Henao-Tamayo M, Ordway D, Sellers RS, Jain P, Chen B, Chen M, Kim J, Lukose R, Chan J, Orme IM, Porcelli SA, Jacobs WR, Jr..** 2011. A recombinant *Mycobacterium smegmatis* induces potent bactericidal immunity against *Mycobacterium tuberculosis*. Nat. Med. **17:**1261–1268. http://dx.doi.org/10.1038/nm.2420.
15. **Ilghari D, Lightbody KL, Veverka V, Waters LC, Muskett FW, Renshaw PS, Carr MD.** 2011. Solution structure of the *Mycobacterium tuberculosis* EsxG-EsxH complex: functional implications and comparisons with other *M. tuberculosis* Esx family complexes. J. Biol. Chem. **286:**29993–30002. http://dx.doi.org/10.1074/jbc.M111.248732.
16. **Abdallah AM, Bestebroer J, Savage ND, de Punder K, van Zon M, Wilson L, Korbee CJ, van der Sar AM, Ottenhoff TH, van der Wel NN, Bitter W, Peters PJ.** 2011. Mycobacterial secretion systems ESX-1 and ESX-5 play distinct roles in host cell death and inflammasome activation. J. Immunol. **187:**4744–4753. http://dx.doi.org/10.4049/jimmunol.1101457.
17. **Daleke MH, Cascioferro A, de Punder K, Ummels R, Abdallah AM, van der Wel N, Peters PJ, Luirink J, Manganelli R, Bitter W.** 2011. Conserved Pro-Glu (PE) and Pro-Pro-Glu (PPE) protein domains target LipY lipases of pathogenic mycobacteria to the cell surface via the ESX-5 pathway. J. Biol. Chem. **286:**19024–19034. http://dx.doi.org/10.1074/jbc.M110.204966.
18. **Mehra A, Zahra A, Thompson V, Sirisaengtaksin N, Wells A, Porto M, Koster S, Penberthy K, Kubota Y, Dricot A, Rogan D, Vidal M, Hill DE, Bean AJ, Philips JA.** 2013. *Mycobacterium tuberculosis* type VII secreted effector EsxH targets host ESCRT to impair trafficking. PLoS Pathog. **9:**e1003734. http://dx.doi.org/10.1371/journal.ppat.1003734.
19. **Serafini A, Pisu D, Palu G, Rodriguez GM, Manganelli R.** 2013. The ESX-3 secretion system is necessary for iron and zinc homeostasis in *Mycobacterium tuberculosis*. PLoS One **8:**e78351. http://dx.doi.org/10.1371/journal.pone.0078351.
20. **Sassetti CM, Boyd DH, Rubin EJ.** 2003. Genes required for mycobacterial growth defined by high density mutagenesis. Mol. Microbiol. **48:** 77–84. http://dx.doi.org/10.1046/j.1365-2958.2003.03425.x.
21. **Rodriguez GM, Voskuil MI, Gold B, Schoolnik GK, Smith I.** 2002. *ideR*, an essential gene in *Mycobacterium tuberculosis*: role of IdeR in iron-dependent gene expression, iron metabolism, and oxidative stress response. Infect. Immun. **70:**3371–3381. http://dx.doi.org/10.1128/IAI.70.7.3371-3381.2002.
22. **Maciag A, Dainese E, Rodriguez GM, Milano A, Provvedi R, Pasca MR, Smith I, Palù G, Riccardi G, Manganelli R.** 2007. Global analysis of the *Mycobacterium tuberculosis* Zur (FurB) regulon. J. Bacteriol. **189:**730–740. http://dx.doi.org/10.1128/JB.01190-06.
23. **Ratledge C, Dover LG.** 2000. Iron metabolism in Pathogenic Bacteria. Annu. Rev. Microbiol. **54:**881–941. http://dx.doi.org/10.1146/annurev.micro.54.1.881.
24. **Ratledge C, Ewing M.** 1996. The occurrence of carboxymycobactin, the siderophore of pathogenic mycobacteria, as a second extracellular siderophore in *Mycobacterium smegmatis*. Microbiology **142:**2207–2212. http://dx.doi.org/10.1099/13500872-142-8-2207.
25. **Rodriguez GM.** 2006. Control of iron metabolism in *Mycobacterium tuberculosis*. Trends Microbiol. **14:**320–327. http://dx.doi.org/10.1016/j.tim.2006.05.006.
26. **Jones CM, Niederweis M.** 2010. Role of porins in iron uptake by *Mycobacterium smegmatis*. J. Bacteriol. **192:**6411–6417. http://dx.doi.org/10.1128/JB.00986-10.
27. **Tullius MV, Harmston CA, Owens CP, Chim N, Morse RP, McMath LM, Iniguez A, Kimmey JM, Sawaya MR, Whitelegge JP, Horwitz MA, Goulding CW.** 2011. Discovery and characterization of a unique mycobacterial heme acquisition system. Proc. Natl. Acad. Sci. U. S. A. **108:** 5051–5056. http://dx.doi.org/10.1073/pnas.1009516108.
28. **Jones CM, Niederweis M.** 2011. *Mycobacterium tuberculosis* can utilize heme as an iron source. J. Bacteriol. **193:**1767–1770. http://dx.doi.org/10.1128/JB.01312-10.
29. **Bitter W, Houben EN, Bottai D, Brodin P, Brown EJ, Cox JS, Derbyshire K, Fortune SM, Gao LY, Liu J, Gey van Pittius NC, Pym AS, Rubin EJ, Sherman DR, Cole ST, Brosch R.** 2009. Systematic genetic nomenclature for type VII secretion systems. PLoS Pathog. **5:**e1000507. http://dx.doi.org/10.1371/journal.ppat.1000507.
30. **Abdallah AM, Gey van Pittius NC, Champion PA, Cox J, Luirink J, Vandenbroucke-Grauls CM, Appelmelk BJ, Bitter W.** 2007. Type VII secretion—mycobacteria show the way. Nat. Rev. Microbiol. **5:**-883–891. http://dx.doi.org/10.1038/nrmicro1773.
31. **Champion PA, Cox JS.** 2007. Protein secretion systems in Mycobacteria. Cell. Microbiol. **9:**1376–1384. http://dx.doi.org/10.1111/j.1462-5822.2007.00943.x.
32. **Simeone R, Bottai D, Brosch R.** 2009. ESX/type VII secretion systems and their role in host-pathogen interaction. Curr. Opin. Microbiol. **12:**4–10. http://dx.doi.org/10.1016/j.mib.2008.11.003.
33. **MacGurn JA, Raghavan S, Stanley SA, Cox JS.** 2005. A non-RD1 gene cluster is required for Snm secretion in *Mycobacterium tuberculosis*. Mol. Microbiol. **57:**1653–1663. http://dx.doi.org/10.1111/j.1365-2958.2005.04800.x.
34. **Fortune SM, Jaeger A, Sarracino DA, Chase MR, Sassetti CM, Sherman DR, Bloom BR, Rubin EJ.** 2005. Mutually dependent secretion of proteins required for mycobacterial virulence. Proc. Natl. Acad. Sci. U. S. A. **102:**10676–10681. http://dx.doi.org/10.1073/pnas.0504922102.

35. **Brodin P, Majlessi L, Marsollier L, de Jonge MI, Bottai D, Demangel C, Hinds J, Neyrolles O, Butcher PD, Leclerc C, Cole ST, Brosch R.** 2006. Dissection of ESAT-6 system 1 of *Mycobacterium tuberculosis* and impact on immunogenicity and virulence. Infect. Immun. **74:**88–98. http://dx.doi.org/10.1128/IAI.74.1.88-98.2006.
36. **Converse SE, Cox JS.** 2005. A protein secretion pathway critical for *Mycobacterium tuberculosis* virulence is conserved and functional in *Mycobacterium smegmatis*. J. Bacteriol. **187:**1238–1245. http://dx.doi.org/10.1128/JB.187.4.1238-1245.2005.
37. **Gao LY, Guo S, McLaughlin B, Morisaki H, Engel JN, Brown EJ.** 2004. A mycobacterial virulence gene cluster extending RD1 is required for cytolysis, bacterial spreading and ESAT-6 secretion. Mol. Microbiol. **53:** 1677–1693. http://dx.doi.org/10.1111/j.1365-2958.2004.04261.x.
38. **Guinn KM, Hickey MJ, Mathur SK, Zakel KL, Grotzke JE, Lewinsohn DM, Smith S, Sherman DR.** 2004. Individual RD1-region genes are required for export of ESAT-6/CFP-10 and for virulence of *Mycobacterium tuberculosis*. Mol. Microbiol. **51:**359–370. http://dx.doi.org/10.1046/j.1365-2958.2003.03844.x.
39. **Hsu T, Hingley-Wilson SM, Chen B, Chen M, Dai AZ, Morin PM, Marks CB, Padiyar J, Goulding C, Gingery M, Eisenberg D, Russell RG, Derrick SC, Collins FM, Morris SL, King CH, Jacobs WR, Jr..** 2003. The primary mechanism of attenuation of bacillus Calmette-Guerin is a loss of secreted lytic function required for invasion of lung interstitial tissue. Proc. Natl. Acad. Sci. U. S. A. **100:**12420–12425. http://dx.doi.org/10.1073/pnas.1635213100.
40. **Stanley SA, Raghavan S, Hwang WW, Cox JS.** 2003. Acute infection and macrophage subversion by *Mycobacterium tuberculosis* require a specialized secretion system. Proc. Natl. Acad. Sci. U. S. A. **100:**-13001–13006. http://dx.doi.org/10.1073/pnas.2235593100.
41. **Ohol YM, Goetz DH, Chan K, Shiloh MU, Craik CS, Cox JS.** 2010. *Mycobacterium tuberculosis* MycP1 protease plays a dual role in regulation of ESX-1 secretion and virulence. Cell Host Microbe **7:**210–220. http://dx.doi.org/10.1016/j.chom.2010.02.006.
42. **Bottai D, Majlessi L, Simeone R, Frigui W, Laurent C, Lenormand P, Chen J, Rosenkrands I, Huerre M, Leclerc C, Cole ST, Brosch R.** 2011. ESAT-6 secretion-independent impact of ESX-1 genes *espF* and *espG1* on virulence of *Mycobacterium tuberculosis*. J. Infect. Dis. **203:**1155–1164. http://dx.doi.org/10.1093/infdis/jiq089.
43. **Garces A, Atmakuri K, Chase MR, Woodworth JS, Krastins B, Rothchild AC, Ramsdell TL, Lopez MF, Behar SM, Sarracino DA, Fortune SM.** 2010. EspA acts as a critical mediator of ESX1-dependent virulence in *Mycobacterium tuberculosis* by affecting bacterial cell wall integrity. PLoS Pathog. **6:**e1000957. http://dx.doi.org/10.1371/journal.ppat.1000957.
44. **Chen JM, Zhang M, Rybniker J, Basterra L, Dhar N, Tischler AD, Pojer F, Cole ST.** 2013. Phenotypic profiling of *Mycobacterium tuberculosis* EspA point mutants reveals blockage of ESAT-6 and CFP-10 secretion *in vitro* does not always correlate with attenuation of virulence. J. Bacteriol. **195:**5421–5430. http://dx.doi.org/10.1128/JB.00967-13.
45. **Addona TA, Shi X, Keshishian H, Mani DR, Burgess M, Gillette MA, Clauser KR, Shen D, Lewis GD, Farrell LA, Fifer MA, Sabatine MS, Gerszten RE, Carr SA.** 2011. A pipeline that integrates the discovery and verification of plasma protein biomarkers reveals candidate markers for cardiovascular disease. Nat. Biotechnol. **29:**635–643. http://dx.doi.org/10.1038/nbt.1899.
46. **Gillette MA, Carr SA.** 2013. Quantitative analysis of peptides and proteins in biomedicine by targeted mass spectrometry. Nat. Methods **10:** 28–34. http://dx.doi.org/10.1038/nmeth.2309.
47. **Griffin JE, Gawronski JD, Dejesus MA, Ioerger TR, Akerley BJ, Sassetti CM.** 2011. High-resolution phenotypic profiling defines genes essential for mycobacterial growth and cholesterol catabolism. PLoS Pathog. **7:**e1002251. http://dx.doi.org/10.1371/journal.ppat.1002251.
48. **Zhang YJ, Ioerger TR, Huttenhower C, Long JE, Sassetti CM, Sacchettini JC, Rubin EJ.** 2012. Global assessment of genomic regions required for growth in *Mycobacterium tuberculosis*. PLoS Pathog. **8:**e1002946. http://dx.doi.org/10.1371/journal.ppat.1002946.
49. **Sassetti CM, Rubin EJ.** 2003. Genetic requirements for mycobacterial survival during infection. Proc. Natl. Acad. Sci. U. S. A. **100:**-12989–12994. http://dx.doi.org/10.1073/pnas.2134250100.
50. **Wagner JM, Evans TJ, Chen J, Zhu H, Houben EN, Bitter W, Korotkov KV.** 2013. Understanding specificity of the mycosin proteases in ESX/type VII secretion by structural and functional analysis. J. Struct. Biol. **184:** 115–128. http://dx.doi.org/10.1016/j.jsb.2013.09.022.
51. **Solomonson M, Huesgen PF, Wasney GA, Watanabe N, Gruninger RJ, Prehna G, Overall CM, Strynadka NC.** 2013. Structure of the mycosin-1 protease from the mycobacterial ESX-1 protein type VII secretion system. J. Biol. Chem. **288:**17782–17790. http://dx.doi.org/10.1074/jbc.M113.462036.
52. **McCann JR, McDonough JA, Pavelka MS, Braunstein M.** 2007. Beta-lactamase can function as a reporter of bacterial protein export during *Mycobacterium tuberculosis* infection of host cells. Microbiology **153:** 3350–3359. http://dx.doi.org/10.1099/mic.0.2007/008516-0.
53. **Champion MM, Williams EA, Kennedy GM, Champion PA.** 2012. Direct detection of bacterial protein secretion using whole colony proteomics. Mol. Cell. Proteomics **11:**596–604. http://dx.doi.org/10.1074/mcp.M112.017533.
54. **Wei JR, Krishnamoorthy V, Murphy K, Kim JH, Schnappinger D, Alber T, Sassetti CM, Rhee KY, Rubin EJ.** 2011. Depletion of antibiotic targets has widely varying effects on growth. Proc. Natl. Acad. Sci. U. S. A. **108:** 4176–4181. http://dx.doi.org/10.1073/pnas.1018301108.
55. **Bottai D, Di Luca M, Majlessi L, Frigui W, Simeone R, Sayes F, Bitter W, Brennan MJ, Leclerc C, Batoni G, Campa M, Brosch R, Esin S.** 2012. Disruption of the ESX-5 system of *Mycobacterium tuberculosis* causes loss of PPE protein secretion, reduction of cell wall integrity and strong attenuation. Mol. Microbiol. **83:**1195–1209. http://dx.doi.org/10.1111/j.1365-2958.2012.08001.x.
56. **Teutschbein J, Schumann G, Möllmann U, Grabley S, Cole ST, Munder T.** 2009. A protein linkage map of the ESAT-6 secretion system 1 (ESX-1) of *Mycobacterium tuberculosis*. Microbiol. Res. **164:**-253–259. http://dx.doi.org/10.1016/j.micres.2006.11.016.
57. **Daleke MH, van der Woude AD, Parret AH, Ummels R, de Groot AM, Watson D, Piersma SR, Jiménez CR, Luirink J, Bitter W, Houben EN.** 2012. Specific chaperones for the type VII protein secretion pathway. J. Biol. Chem. **287:**31939–31947. http://dx.doi.org/10.1074/jbc.M112.397596.
58. **Chen JM, Zhang M, Rybniker J, Boy-Röttger S, Dhar N, Pojer F, Cole ST.** 2013. *Mycobacterium tuberculosis* EspB binds phospholipids and mediates EsxA-independent virulence. Mol. Microbiol. **89:**1154–1166. http://dx.doi.org/10.1111/mmi.12336.
59. **Champion PA, Champion MM, Manzanillo P, Cox JS.** 2009. ESX-1 secreted virulence factors are recognized by multiple cytosolic AAA ATPases in pathogenic mycobacteria. Mol. Microbiol. **73:**950–962. http://dx.doi.org/10.1111/j.1365-2958.2009.06821.x.
60. **McLaughlin B, Chon JS, MacGurn JA, Carlsson F, Cheng TL, Cox JS, Brown EJ.** 2007. A mycobacterium ESX-1-secreted virulence factor with unique requirements for export. PLoS Pathog. **3:**e105. http://dx.doi.org/10.1371/journal.ppat.0030105.
61. **Houben EN, Bestebroer J, Ummels R, Wilson L, Piersma SR, Jiménez CR, Ottenhoff TH, Luirink J, Bitter W.** 2012. Composition of the type VII secretion system membrane complex. Mol. Microbiol. **86:**-472–484. http://dx.doi.org/10.1111/j.1365-2958.2012.08206.x.
62. **Festa RA, McAllister F, Pearce MJ, Mintseris J, Burns KE, Gygi SP, Darwin KH.** 2010. Prokaryotic ubiquitin-like protein (Pup) proteome of *Mycobacterium tuberculosis* [corrected]. PLoS One **5:**e8589. http://dx.doi.org/10.1371/journal.pone.0008589.
63. **Farhana A, Kumar S, Rathore SS, Ghosh PC, Ehtesham NZ, Tyagi AK, Hasnain SE.** 2008. Mechanistic insights into a novel exporter-importer system of *Mycobacterium tuberculosis* unravel its role in trafficking of iron. PLoS One **3:**e2087. http://dx.doi.org/10.1371/journal.pone.0002087.
64. **Rodriguez GM, Smith I.** 2006. Identification of an ABC transporter required for iron acquisition and virulence in *Mycobacterium tuberculosis*. J. Bacteriol. **188:**424–430. http://dx.doi.org/10.1128/JB.188.2.424-430.2006.
65. **Ryndak MB, Wang S, Smith I, Rodriguez GM.** 2009. *Mycobacterium tuberculosis* high affinity iron importer, IrtA, contains an FAD-binding domain. J. Bacteriol. **192:**861–869. http://dx.doi.org/10.1128/JB.00223-09.